International Journal on Recent and Innovation Trends in Computing and Communication
ISSN: 2321-8169 Volume: 11 Issue: 11s
DOI: https://doi.org/10.17762/ijritcc.v11i11s.8168
***Article Received:** 28 June 2023 **Revised:** 25 August 2023 **Accepted:** 10 September 2023*

Wave-Atom and Cycle-Spinning-Based Noise Reduction in Mammography Images

Dr. Ch. Sarada[1], P. Ashwini[2], K. Srividya[3]
[1]Department of CSE, CVR College of Engineering, Hyderbad, India
chintala.sarada@cvr.ac.in
[2]Department of CSE, VASAVI College of Engineering, Hyderbad, India
ashwinireddy90@gmail.com
[3]Department of CSE, VASAVI college of Engineering, Hyderbad, India
ksrividya0508@gmail.com

Abstract— Image denoising is crucial in medical image processing. Digital mammography depends significantly on de-noising for computer-aided-detection of malignant cells like Microcalcifications. In this work, we proposed an unique hybrid approach to reduce Gaussian noise in digital mammograms by combining the wave-atom translation and cycle spinning methods. Pictures denoised by thresholding of coefficients would produce pseudo-Gibbs events because wave atoms are not translationally invariant. Circular motion is applied to keep away the artefacts. Experimental results clearly establish that the method is effective at filtering out background noise while maintaining the integrity of edges and enhancing picture quality. Mini-Mias pictures with variable quantities of Gaussian Noise are used to evaluate and analyse the performance using peak signal-to-noise ratio and structural similarity index. The provided technique outperforms several current filters in terms of evaluated results of peak signal-to-noise ratio and structural similarity index.

Keywords- Mammogram; denoising framework; wave atoms; thresholding; translation invariance; Cycle Spinning; peak signal-to-noise ratio (PSNR) ; structural similarity index(SSIM)

I. INTRODUCTION

Amidst the various female cancers, Breast cancer is both the most prevalent and deadly [1]. Breast cancer has been the second most common disease in Human Beings. Among women, Breast cancer had the highest incidence rate and its mortality rate is high. Among women above 40 years age , cancer is the biggest cause of death[2]. Preventing Breast cancer is difficult since its precise causes are yet unclear [3]. Yet, with prompt medical attention, one's chances of survival could well be enhanced. When it comes to screening for Breast cancer, Mammography is both the most effective and reliable screening modality [3, 4].

Mammography is a screening and diagnostic procedure that examines the human Breast organ using low-energy X-rays [4,28]. This Mammography test is mainly intended to detect Microcalcifications and Masses within the Breast organ[5,30], allowing for early identification of Breast cancer. Cancer has a 30% chance of being cured if caught early, but only a 5% chance if the tumor has progressed to an advanced stage [6, 7].However, X-ray pictures often suffer from degradation owing to a number of causes[29]. In particular, abnormalities linked to picture noise reduce the detection effectiveness of standard 2-D mammography, making it difficult to make an accurate diagnosis of calcification or a tiny tumor, for example. The median filter, adaptive median filter, and Wiener filter [8,9], have been used to minimise the noise in images.

Noise, such as gaussian noise, will reduce the image's overall quality by adding unanticipated random values to the original data during the capturing or transmitting process. The image quality of a Mammogram must be enhanced via multiple stages of the preprocessing pipeline before it can be utilized for diagnostic purposes. So, in the preprocessing step of the computer aided diagnosis system for identifying Breast cancer, noise reduction plays a crucial role. For proper analysis, picture rebuilding methods are required. Image denoising is a very important part of the restoration process. Noise can be eliminated using either the spatial domain or the frequency domain. Spatial domain methods may alter pixel intensities in image domain [1] by combining a picture with a filter function called the kernel. To accomplish the similar streaming effect in the frequency domain, a convolution with this kernel incurs a considerable computational cost compared to the cost of conducting a multiplication operation[26,27]. One of the primary advantages of the transform domain techniques is that in contrast to conventional filters, transform domain methods enable time and frequency-domain localization at the same time[25]. Its strength lies in their capacity to separate various aspects of a signal. This may help to sharpen the image while also reducing noise. Another benefit is that it can clean un-wanted noise from images while keeping details sharp and edges sharp. This is because it can break down an image into its frequency components, allowing for a more in-depth

International Journal on Recent and Innovation Trends in Computing and Communication
ISSN: 2321-8169 Volume: 11 Issue: 11s
DOI: https://doi.org/10.17762/ijritcc.v11i11s.8168
***Article Received:** 28 June 2023 **Revised:** 25 August 2023 **Accepted:** 10 September 2023*

examination. Because of their effectiveness in minimizing noise while maintaining finer details, transform domain techniques are a powerful mechanism for image restoration.

Sparsely and effectively representing pictures might need a variety of transformations[25,26]. It turns out that the statistical properties of the wavelet transform coefficients of natural images make them a useful resource for denoising images[10]. Denoising Mammographic images using a wavelet-domain approach is proposed by Lashari et al. [11]. As an alternative to wavelets, many geometric transformations have been proposed that provide precise reconstruction of edges and texture areas. Examples of such transformations are curvelets [12] and wave atoms [13]. In order for these transforms to be used for denoising, a threshold must be chosen that is uniformly applied to all of the transform's coefficients. An alternative approach includes picking a different threshold for each level of the revised coefficients [14].

Throughout the last several years, picture denoising has been dominated by the approach of shrinking and thresholding the coefficients of the wavelet transform. Yet, the singularities of lines and curves cannot be captured by the wavelets' isotropic basis elements. In contrast to the wavelet transform[12], the curvelet transform is superior at displaying edges and singularities along curves, but it fails to capture the pattern across the oscillations. The oscillatory basis functions of wave atoms provide a sparser expansion and a better representation than wavelets or curvelets, but at the cost of creating artefacts in the homogenous portions of the image, which results in the pseudo-Gibbs phenomena.

The Cycle Spinning [15] technique is a viable treatment for the pseudo-Gibbs effect. In this research, we suggest combining the Cycle Spinning method with a new wave atom thresholding approach to effectively remove noise without damaging the image's edges or finer details. The ideas of wave atom transformation and cycle spinning are discussed at length in Section 2 of this book. Section 4 contains actual data and discussion, whereas Section 3 lays out the theoretical background for thresholding of wave atom denoising. Section 5 contains the conclusion.

II. MATERIALS AND METHODS

A. Gaussian noise model

Digital pictures with noise reveal undesirable details. Artifacts, false edges, invisible lines, corners, fuzzy objects and jarring backdrop sceneries are some of the negative outcomes of noise. The probability density function of Gaussian Noise is equivalent to the normal distribution's, often known as the Gaussian Distribution. Natural sources of Gaussian noise [16] include thermal oscillation of atoms and the intermittent character of radiation from hot objects. The grayscale values of digital photographs are often distorted by Gaussian noise. To this end, the normalised histogram of a Gaussian noise model is used to characterise its key design and properties and it is given as:

$$P(v) = \sqrt{\frac{1}{2\pi\sigma^2}} e^{-\frac{(v-\mu)^2}{2\sigma^2}} \quad (1)$$

In most cases, the mathematical model of Gaussian noise is a good representation of the actual world. The bell-shaped distribution of normalised Gaussian noise is a consequence of this uniform unpredictability. As can be seen in figure 1, the probability distribution follows a bell shape with a mean of 0 and a standard deviation of 1 .

Figure 1. Plot of Probability Distribution Function

B. Wave Atom Transform

Wave atoms comes from a rare formulation of wave equations. Two-dimensional wave atoms are a special case of a wavelet packet where scaling of support and wavelength happens according to a parabolic function. Using the tensor product of one-dimensional wave packets, as described in Lars Villemoes' frequency domain localization technique [17,18], we build the wave atoms basis function $\psi_{a,b}^{j}(x)$. Wave atoms transformation is realised via convolution interpolation between the basis functions of the picture and the wave atoms, yielding the image wave atoms coefficients [19,31].The transformation of atoms' space-time waves in one dimension can be written as:

$$P_{j,a,b} = \int \psi_a^j(x - 2^{-j}b)k(x)dx = \psi_a^j(x - 2^{-j}b) * k(x) \quad (2)$$

where Pj,a,b denotes wave atoms coefficients, k(x) denotes one-dimensional input data, j denotes scale, a and b denotes integer values.

C. Cycle Spinning

If the transformation used in the threshold denoising process lacks translation invariance, distortion will be introduced into the picture in the neighborhood of discontinuous points (edges and textures); this distortion is very dependent on the position of the image's discontinuous points. Image translation, followed by noise reduction at a thresholding level on the translated picture, and finally reverse translation of the denoised image,

International Journal on Recent and Innovation Trends in Computing and Communication
ISSN: 2321-8169 Volume: 11 Issue: 11s
DOI: https://doi.org/10.17762/ijritcc.v11i11s.8168
***Article Received:** 28 June 2023 **Revised:** 25 August 2023 **Accepted:** 10 September 2023*

can be done to prevent the pseudo-Gibbs phenomena. Nevertheless, if the picture to be examined has many discontinuous points, finding a translation amount that can satisfy the needs of all discontinuous points might be challenging. This is because the best translation of one discontinuous point may intensify the pseudo-Gibbs phenomena of another discontinuous point's surrounding region. Coifman and Donoho introduced Cycle Spinning technology[15], which entails doing "cycle spinning-threshold denoising-reverse cycle spinning" in order to prevent the pseudo-Gibbs phenomena that arises from the threshold denoising process's lack of translation invariance. The mathematical expression for a single spin cycle is:

$$S_{i,j}(f_{x,y}) = f_{(i+x,j+y)modg1,g2}$$
$$S_{-i,-j}(f_{x,y}) = f_{(-i+x,-j+y)modg1,g2} \quad (3)$$

where $S_{i,j}$ indicates a 2-D circular shift, s-i,-j represents a 2-D reverse circular shift, i and j indicate the amount of change in the horizontal and vertical axes. g1 stands for the horizontal dimensions of a picture and g2 stands for the vertical dimension. To prevent the pseudo-Gibbs phenomenon from occurring in the same location after each translation, we do not employ a single translation but rather acquire a new denoising result $\hat{u}_{i,j}$ for each translation in the image's rows and columns, with the resulting denoising result $\hat{u}_{C1,C2}$ being a linear average of the previous results. $\hat{u}_{i,j}$ $\hat{u}_{C1,C2}$ are formulated as:

$$\hat{u}_{i,j} = S_{-i,-j}(W^{-1}(\mathrm{T}[W(S_{i,j}(x))]),$$
$$\hat{u}_{C1,C2} = \frac{1}{C_1 C_2}\sum_{i=0}^{C_1}\sum_{j=0}^{C_2}\hat{u}_{i,j}. \quad (4)$$

Here, C1, C2 is the maximum row and column translation amount, $S_{i,j}$ is the cycle spinning operator, W is the transformation operator and W^{-1} is its inverse operator and T is the threshold operator.

III. WAVE ATOM THRESHOLD FUNCTION FOR GAUSSIAN NOISE REDUCTION IN MAMMOGRAMS

Wavelet-based denoising is congruent with the fundamental principle of threshold denoising based on wave atoms transformation. Signal processing applications often display high-frequency noise signals while low-frequency or smoother usable signals are shown. Noise can be removed from signals by first decomposing them into wave atoms and then reconstructing them using threshold quantization threshold processing on the high frequency wave atom coefficients. When the one-dimensional signal has been decomposed using wave atom decomposition, the high-frequency coefficients of wave atom decomposition are quantified and the reconstructed one-dimensional wave atom is then subjected to a denoising procedure. Both the denoising threshold and the chosen threshold function are crucial in determining the final denoising quality.

Traditional Threshold Function: The hard criterion operation retains its decomposition value that is larger than the criterion value and sets the value to zero if it is lower than the criterion value over a range of scale-spaces. [19]. The signal's local features are preserved; however, the approach introduces some noise into the reconstructed signal due to the discontinuity. Traditional threshold function expression is:

$$P_T = \begin{cases} 0; & |P_r| \le T_j \\ P_r; & |P_r| > T_j' \end{cases} \quad (5)$$

Setting the criterion value of the decomposition value to zero is the goal of the soft threshold function. Coherence is preserved in the decomposition value after the technique, although certain high frequency values above the threshold are lost [20]. Soft threshold function expression is:

$$P_T = \begin{cases} 0; & |P_r| \le T_j \\ \mathrm{sgn}(P_r)(|P_r| - T_j); & |P_r| > T_j' \end{cases} \quad (6)$$

where predicted wavelet values are represented by P_T, decomposed wavelet values by P_r, threshold at level j by T_j and the symbolic piecewise function by sgn(*) [21,22].

The Enhanced Threshold Operation: Soft threshold functions have superior continuity. To overcome the limitations of soft and hard threshold operations, a new threshold function, semisoft which is compromised between hard and soft is proposed, the expression is :

$$P_T = \begin{cases} 0; & |P_r| \le T_j \\ \mathrm{sgn}(P_r)(|P_r| - KT_j); & |P_r| > T_j' \end{cases} \quad (7)$$

Among soft and hard threshold functions, T is defined between 0 and 1. Despite a semisoft threshold function result between 0 and 1, T remains fixed. Therefore, fixed bias still exists. So, to have more adaptability, a complex exponential function is proposed for K as follows:

$$\mathrm{K} = \exp^{-5}[(|P_r| - T_j)/T_j] \quad (8)$$

Where, when $|P_r| = T_j$, $P_T = 0$ and when $|P_r| \to T_j$, $P_T \to 0$. Therefore, the enhanced threshold function has the properties of soft threshold function. When $|P_r| \to \infty$, $P_T \to P_r$ enhanced threshold function based on $P_T = P_r$ as the asymptotic line. It can be observed that as P_r becomes larger, P_T converges on. When P_r becomes infinite, the two values are about equivalent. As a result, the new threshold function combines the best features of the hard and soft threshold functions to eliminate the drawbacks of both. Therefore, this threshold function is preferable for improving the denoising impact.

International Journal on Recent and Innovation Trends in Computing and Communication
ISSN: 2321-8169 Volume: 11 Issue: 11s
DOI: https://doi.org/10.17762/ijritcc.v11i11s.8168
***Article Received:** 28 June 2023 **Revised:** 25 August 2023 **Accepted:** 10 September 2023*

The efficacy of the wavelet threshold denoising process depends heavily on the threshold value T_j, a crucial parameter in the algorithm. Some examples of thresholds [23], includes rigrsure, heursure, sqtwolog, and minimaxi[23]. The constant threshold is often used. The formula for the constant threshold is $T_j = s_n\sqrt{2\ln N}$ where s_n is the standard deviation of the noise and N is the total length of the signal.

The proposed work considers the enhanced constant threshold. Its expression is $T_j = s_n\sqrt{2\ln N}/\log 2(j+1)$. The threshold improvement value decreases monotonically as decomposition scale j is larger. To guarantee efficient de-noising, it is compatible with the noise's propagation properties over the wavelet transform's scales. The expanded useable signal information could be guaranteed by the enhanced threshold approach.

A. Steps in an Image denoising algorithm

step 1. The first step is to utilize the cycle spinning operator to perform cycle spinning on the noisy picture u, yielding the image S(u).

step 2.To calculate the transformation coefficient WS(u), apply two-dimensional atom wave transformation W to the image S(u) after spin it for a cycle.

step 3.Once the noise has been removed, the next step is to convert these coefficients using the suggested threshold operator (let's refer to it as T). This yields the transformation coefficient T(WS(u)).

step 4.To create the denoised picture $W^{-1}(T(WS(u))$, we must first threshold the image, then perform an inverse 2-dimensional transformation of the wave atoms on their coefficient T(WS(u)).

Step 5.By performing spinning in reverse on the denoised picture $W^{-1}(T(WS(u)))$, where S^{-1} denotes the spinning operator in the reverse cycle, we can get the restored image $u = S^{-1}W^{-1}(T(WS(u)))$, and the ultimate denoising results will be calculated by taking a mean of all results.

The operation flow of the proposed technique to eliminate noise and restore the original picture is shown in the figure. 2.

IV. PROPOSED WORK RESULTS AND DISCUSSION

To validate the suggested method, Mammography pictures are used. A total of 322 Mammogram images consisting of conjectured, bounded and ill-defined Masses in Mini-MIAS database [24] are used . Each image is contaminated by adding zero-mean Gaussian noise with various noise deviation σ values(10,20,30,40).

In order to conduct an analysis of the results of the experiment, the Peak signal-to-noise ratio and the structural similarity index are both used. The Peak signal-to-noise ratio is calculated using a mean square error approximation as:

$$MSE = \frac{1}{R_1 R_2}\sum_{i=1}^{R_1}\sum_{j=1}^{R_2}[M_1(i,j) - M_2(i,j)]^2$$
$$PSNR = 10 \times \log\left(\frac{255^2}{MSE}\right) \quad (9)$$

where M_1 and M_2 represent two images of size R1 × R2, $M_1(i, j)$ is the i^{th} row, j^{th} column pixel value of M_1. MSE is the mean square error between two images. Formula for SSIM Index is as shown below:

$$\text{SSIM}\ (M_1, M_2) = \frac{(2\mu_{M_1}\mu_{M_2}+H_1)(2\sigma_{M_1M_2}+H_2)}{(\mu_{M_1}^2+\mu_{M_2}^2+H_1)(\sigma_{M_1}^2+\sigma_{M_2}^2+H_2)} \quad (10)$$

where μ_{M_1} is the mean gray values of M1 and σ_{M_1} is the variance for M1, $\sigma_{M_1M_2}$ correspond to the covariance between the two images M_1 and M_2, and the symbols H_1 and H_2 are two small constants [25]. The Peak signal-to-noise ratio or the structural similarity index is directly proportional to the denoising factor which therefore results in a closer denoised image M2 to the original M1. Tables 1,2,3,4 show the results comparison.

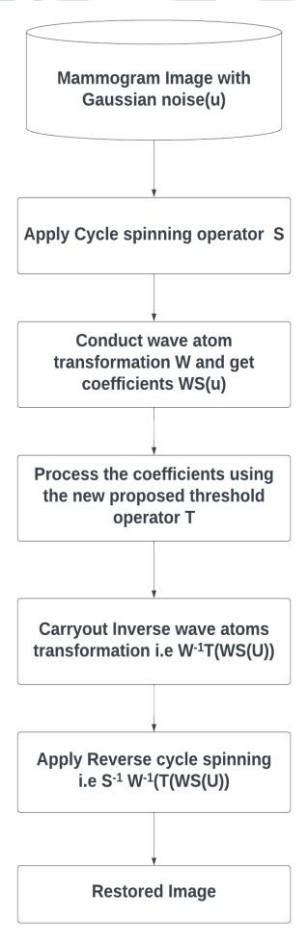

Figure 2. Operation flow of Proposed work for Noise removal

International Journal on Recent and Innovation Trends in Computing and Communication
ISSN: 2321-8169 Volume: 11 Issue: 11s
DOI: https://doi.org/10.17762/ijritcc.v11i11s.8168
***Article Received:** 28 June 2023 **Revised:** 25 August 2023 **Accepted:** 10 September 2023*

Table 1. Result of PSNR and MSE for different thresholds for mdb055 image with 40% percentage of noise ratio

Criterion	Hard Threshold	Soft Threshold	New Threshold
PSNR	36.78	34.76	38.91
MSE (10^{-4})	1.4697	2.6859	0.7231

Table 2. PSNR results of the methods for the mdb055 image with various percentage of noise ratios

Methods	Percentage of noise ratio			
	10%	20%	30%	40%
Standard Median Filter	29.28	19.32	15.84	12.79
Adaptive Median Filter	33.63	24.85	21.29	17.63
Adaptive Bilateral Filter	37.56	30.67	24.72	20.14
Wavelet Denoising	42.12	40.21	37.61	34.58
Proposed (wave atom)	**44.56**	**42.73**	**40.87**	**38.91**

Table 3.SSIM results of the methods for the mdb055 Image with various percentage of noise ratios

Methods	Percentage of noise ratio			
	10%	20%	30%	40%
Standard Median Filter	0.87	0.71	0.56	0.45
Adaptive Median Filter	0.91	0.73	0.62	0.52
Adaptive Bilateral Filter	0.92	0.82	0.71	0.63
Wavelet Denoising	0.94	0.88	0.82	0.74
Proposed (wave atom)	**0.96**	**0.93**	**0.89**	**0.85**

Table 4. Mean PSNR and the mean SSIM values of the approaches for 322 images using different percentage of noise ratios

Algorithm	Criterion	Percentage of noise ratio			
		10%	20%	30%	40%
Standard Median Filter	PSNR	28.76	18.63	14.59	11.68
	SSIM	0.8645	0.7126	0.5762	0.4518
Adaptive Median Filter	PSNR	32.85	23.67	20.32	16.83
	SSIM	0.9023	0.7285	0.6194	0.5246
Adaptive Bilateral Filter	PSNR	36.41	29.83	23.49	19.72
	SSIM	0.9187	0.8234	0.7145	0.6353
Wavelet Denoising	PSNR	41.23	39.86	36.59	33.75
	SSIM	0.9368	0.8821	0.8246	0.7462
Proposed (wave atom)	PSNR	**44.35**	**42.54**	**40.27**	**38.16**
	SSIM	**0.9658**	**0.9265**	**0.8972**	**0.8523**

As can be seen in Tables 2, 3, and 4, proposed technique yielded improved results in picture denoising while retaining the images' structural information, demonstrating promising futuristic use.

A sample image with noise levels of 10%, 20%, 30% ,40% and the corresponding restored images are presented in figures 3,4,5 and 6 respectively.

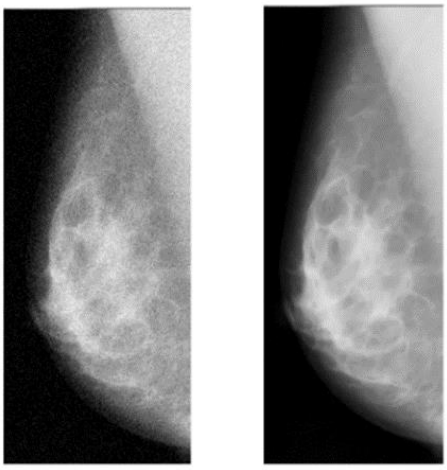

Figure. 3. mdb055 with a noise level of 10% and restored image

Figure. 4.mdb055 with a noise level of 20% and restored image

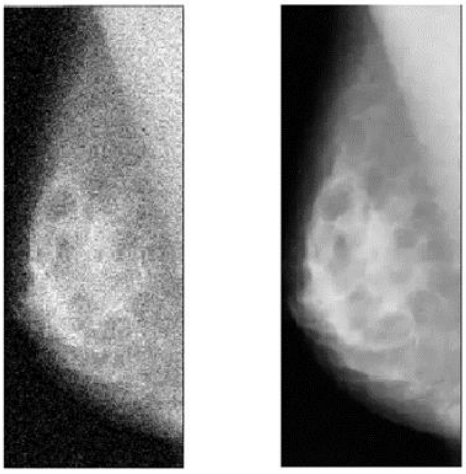

Figure.5.mdb055 with a noise level of 30% and restored image

International Journal on Recent and Innovation Trends in Computing and Communication
ISSN: 2321-8169 Volume: 11 Issue: 11s
DOI: https://doi.org/10.17762/ijritcc.v11i11s.8168
***Article Received:** 28 June 2023 **Revised:** 25 August 2023 **Accepted:** 10 September 2023*

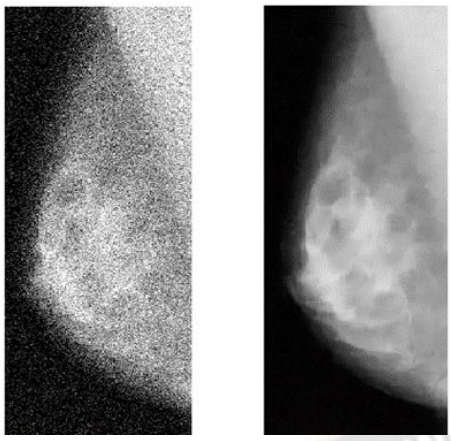

Fig. 6. mdb055 with a noise level of 40% and restored image

V. CONCLUSION

A novel denoising model using a combination of wave atom thresholding and cycle spinning is proposed to remove Gaussian noise from Mammograms. By enhancing the precision of the threshold estimate, the proposed method enhance the denoising effects in Mammograms. The procedure begins with a wave atom transformation, continues with a cycle spinning operation, uses a recommended threshold function to adjust the coefficients and concludes with the application of the inverse wave atom and reverse cycle spinning operators. The proposed method shown improvement in PSNR and reduce MSE in the final image, as well as address the issues of constant deviation and discontinuous function in the hard threshold function and enables different decomposition scales to employ the same threshold value when processing noise. Besides effectively eliminating picture noise, this method also retains the image's edges and textures and prevent the pseudo-Gibbs phenomenon, resulting in a denoised image that appeared more genuine. Evaluation indicators are used to quantify the results after denoising the Mini-Mias dataset. When compared to existing denoising models, the proposed method excels since it not only improves the quality of denoised photographs, but also maintains the detailed structure consistent with the original images. There is further scope to modify the proposed algorithm in the future for effective processing and functionality improvement of real clinical mammography images.

REFERENCES

[1] IARC. World cancer report: International agency for research on cancer. Lyon, 2008

[2] B. W. Stewart, C. P. Wild, World Cancer Report 2014, World Health Organization (2014), 18-20.

[3] DeSantis CE, Ma J, Goding Sauer A, Newman LA, Jemal A(2017). Breast cancer statistics, 2017, racial disparity in mortality by state. CA Cancer J Clin, 67, 439-48.

[4] Sannasi Chakravarthy SR, Rajaguru H (2019). Detectionand classification of microcalcifica- tion from digital mammograms with firefly algorithm, extreme learningmachine and non-linear regression models: A compari-son. Int J Imaging Syst Technol, 2019, 1– 21.

[5] Gøtzsche PC, Nielsen M (2009). Screening for Breast cancer with mammography. Cochrane Database Syst Rev, 4.

[6] Elmore JG, Nakano CY, Koepsell TD, Desnick LM, D'Orsi CJ, Ransohoff DF. International variation in screen-ing mammography interpretations in community-based programs. J Natl Cancer Inst. 2003;95(18):1384–1393.

[7] Veronesi U, Boyle P, Goldhirsch A, Orecchia R, Viale G. Breast cancer. Lancet. 2005;365:1727–1741.

[8] H. Hwang, R. A. Haddad, Adaptive median filters: new algorithms and results, IEEE Transaction on Image Pro-cessing 4 (1995) 499-502.

[9] A. Buades, B. Coll, M. Morel, A review of image denoising algorithms, with a new one, Multiscale Modelling and Simulation 4 (2005) 490-530.

[10] Gonzalez, R.C., Woods, R.E.: Digital Image Processing. 2nd edn. Pearson Education, Singapore (2002)

[11] Lashari, Saima & Ibrahim, Rosziati & Senan, Norhalina. (2015). De-noising analysis of mammogram images in the waveletdomain using hard and soft thresholding. 2014 4th World Congress on Information and Communi-cation Technologies, WICT 2014. 353-357.

[12] Starck, J.L., Candes, E.J., Donoho, D.L.: The curvelet transform for image denoising. In: IEEE Trans. Image Pro-cess. 11(6), 670–684 (2002)

[13] Demanet, L., Ying, L.: Wave atoms and sparsity of oscillatory patterns. Appl. Comput. Harmon. Anal. 23(3), 368–387 (2007)

[14] Swami, P.D., Jain, A., Singhai, J.: A multilevel Shrinkage approach for curvelet denoising. In: Proceeding of International Conference on Information and Multimedia Technology, pp. 268–272, Jeju Island, Korea (Dec. 16–18, 2009)

[15] Coifman R R, Donoho D L. Translation-invariant denoising [A].Lecture Notes in Statistics: Wavelets and Statis-tics. New York: Springer-verlag, 1995: 125- 150.

[16] Boyat, A. and Joshi, B. K. (2013) "Image Denoising using Wavelet Transform and Median Filtering', IEEE Nir-ma University International Conference on Engineering," Ahemdabad.

[17] L.F. Villemoes, Wavelet packets with uniform time-frequency localization, C. R. Acad. Bulg. Sci. 335 (2002) 793–796.

[18] S. Suguna Mallika, D. Rajya Lakshmi, "MUTWEB- A Testing Tool for performing Mutation Testing of Java and Servlet Based Web Applications", International Journal of Innovative Technology and Exploring Engineering, Volume 8, Issue 12, PP:5406-5413, DOI:10.35940/ijitee.L3789.1081219.

[19] L. Demanet, L. Ying, Wave atoms and sparsity of oscillatory patterns, Appl. Comput. Harmon. Anal. 23 (2007) 368–387.

[20] C. He, J. C. Xing, and Q. L. Yang, "Optimal wavelet basis selection for wavelet denoising of structural vibration signal, "Applied Mechanics and Materials, vol. 578-579, pp. 1059–1063, 2014.

[21] J.-Y. Tang, W.-T. Chen, S.-Y. Chen, and W. Zhou, "Wavelet based vibration signal denoising with a new adaptive thresholding function," Journal of Vibration and Shock, vol. 28, no. 7, pp. 118–121, 2009 (Chinese).

International Journal on Recent and Innovation Trends in Computing and Communication
ISSN: 2321-8169 Volume: 11 Issue: 11s
DOI: https://doi.org/10.17762/ijritcc.v11i11s.8168
***Article Received:** 28 June 2023 **Revised:** 25 August 2023 **Accepted:** 10 September 2023*

[22] S. Badiezadegan and R. C. Rose, "A wavelet-based thresholding approach to reconstructing unreliable spectro-gram components," Speech Communication, vol. 67, pp. 129–142, 2015.

[23] [K. L. Yuan, "Wavelet denoising based on threshold optimization method," Engineering Journal of Wuhan Uni-versity, vol. 48, no. 1, pp. 74–80, 2015.

[24] Rama Prabha Krishnamoorthy, Abdul Rahman bin Senathirajah, Robinson Savarimuthu, Abdul Rahim Sadiq Batcha. (2023). An Ultracompact All Optical Two-Dimensional Photonic Crystal Based and Gate. International Journal of Intelligent Systems and Applications in Engineering, 11(4s), 328–333. Retrieved from https://ijisae.org/index.php/IJISAE/article/view/2672.

[25] J. Suckling, "The Mammographic Image Analysis Society Digital Mammogram Database," Exerpta Medica International Congress, Vol. 1069, 1994, pp. 375-378

[26] Z. Wang, A. C. Bovik, H. R. Sheikh, et al., Image quality assessment: from error visibility to structural similarity. IEEE Trans. Image Process. 13(4), 600–612 (2004).

[27] Saini, D. J. B. ., & Qureshi, D. I. . (2021). Feature Extraction and Classification-Based Face Recognition Using Deep Learning Architectures. Research Journal of Computer Systems and Engineering, 2(1), 52:57. Retrieved from https://technicaljournals.org/RJCSE/index.php/journal/article/view/23.

[28] Suguna Mallika S.,A. Sanjana, A. Vani Gayatri and S. Veena Naga Sai, "Sign Language Interpretation Using Deep Learning", Multi-disciplinary Trends in Artificial Intelligence - 16th International Conference, {MIWAI} 2023, Hyderabad, India, July 21-22, 2023, Proceedings, LNCS, 14078, PP-692-703, 10.1007/978-3-031-36402-0_64.

[29] Prof. Bhushan Thakre, Dr. R.M Thakre. (2017). Analysis of Modified Current Controller and its Implementation in Automotive LED. International Journal of New Practices in Management and Engineering, 6(04), 01 - 06. https://doi.org/10.17762/ijnpme.v6i04.60.

[30] S. Suguna Mallika, D. Rajya Lakshmi, "Mutation Testing and Its Analysis on Web Applications for Defect Prevention and Performance Improvement", International Journal of e-Collaboration, Volume 17, Issue 1, PP:71-88 doi: 10.4018/IJeC.2021010105.

[31] Ch.Sarada, C., Lakshmi, K. V. ., & Padmavathamma, M. . (2023). MLO Mammogram Pectoral Masking with Ensemble of MSER and Slope Edge Detection and Extensive Pre-Processing. International Journal on Recent and Innovation Trends in Computing and Communication, 11(3), 135–144. https://doi.org/10.17762/ijritcc.v11i3.6330.

[32] C. Sarada, V. Dattatreya and K. V. Lakshmi, "Deep Learning based Breast Image Classification Study for Cancer Detection," 2023 IEEE International Conference on Integrated Circuits and Communication Systems (ICICACS), Raichur, India, 2023, pp. 01-08, doi: 10.1109/ICICACS57338.2023.10100206.

[33] C. Sarada, K. V. Lakshmi and M. Padmavathamma, "Spatial Intuitionistic Fuzzy C-means with Calcifications enhancement based on Nonsubsampled Shearlet Transform to detect Masses and Microcalcifications from MLO Mammograms," 2023 Advanced Computing and Communication Technologies for High Performance Applications (ACCTHPA), Ernakulam, India, 2023, pp. 1-10, doi: 10.1109/ACCTHPA57160.2023.10083338.

[34] Pappula Madhavi, Supreethi K P (2022), "STAQR Tree indexing for spatial temporal data with altitude", GIS Science Journal, ISSN NO: 1869-9391, online open access publication in GS Journal Volume 9, Issue 11, 2022.https://doi.org/10.21203 .